

DUCT VELOCITY PROFILES AND THE PLACEMENT OF AIR CONTROL SENSORS

E.I. Griggs, Ph.D., P.E.
Member ASHRAE

W.B. Swim, Ph.D., P.E.
Member ASHRAE

H.G. Yoon

ABSTRACT

Pitot tubes were used to determine air velocities downstream of 69 sheet metal duct fittings, including elbows, conical contractions, conical diffusers, round-to-round junctions, and rectangular-to-round junctions. For target mass-average velocities of 1000 and 2500 fpm, centerline velocities were measured at distances of 1, 2, 4, 6, and 10 diameters downstream of the fittings. Vertical and horizontal velocity profiles were obtained at the same stations for a target mass-average velocity of 1750 fpm. For junctions, measurements were made over a range of main-to-branch flow rate ratios. For one elbow and two tees, profiles were also obtained at downstream distances larger than 10 diameters.

Results are expressed as the ratio of measured velocity to average velocity. Flow is not fully developed for any case. Flow rate calculations using profile data for 20 cases yield large errors at 1 diameter downstream of any fitting; however, the error is significantly lower at the 10-diameter station. Typical vertical and horizontal profiles at each measuring station are shown graphically. Measured centerline velocities are tabulated.

The identification of the velocity profiles leaving these fittings is of particular importance in locating VAV terminal units within a duct system. The control accuracies of these terminals cannot be expected to be any greater than the accuracy of measurement of the parameter they are controlling, in this case velocity or velocity pressure. The data obtained in this study offer valuable information regarding the optimal location of these measuring and controlling devices, as well as the expected accuracies of measurement and, thus, control.

INTRODUCTION

The primary objective of the work reported in this paper was to measure centerline velocity at distances of 1, 2, 4, 6, and 10 diameters (D) downstream of 69 HVAC sheet metal duct fittings including elbows, conical contractions, conical diffusers, round-to-round junctions, and rectangular-to-round junctions. Only centerline velocities were measured for target mass-average velocities of 1000 and 2500 fpm, while velocity profiles were obtained via traverses for a target mass-average velocity of 1750 fpm. Detailed descriptions of the work, a complete listing of all data, and plots of vertical and horizontal profiles are given in Griggs et al. (1987).

A secondary objective of this study was to apply the data obtained through the testing phase to predict optimal location of singlepoint flow-measuring devices and to estimate the relative accuracy that might be expected under optimal and less than optimal, but more realistic, conditions. Although most pneumatically controlled terminal units currently utilize some type of flow-averaging sensor with multiple pick-up points, many electronically controlled units still offer only a single-point pick-up. This collection of data, obtained at various distances downstream from the fittings and at various main/branch duct velocities, enables certain conclusions to be formed regarding the selection of optimal sensor locations and identifies limitations of the single-point sensor accuracy when subjected to certain take-off and operational conditions. The data do not cover velocity patterns from disturbances such as dampers and flexible duct.

EXPERIMENTAL SYSTEM

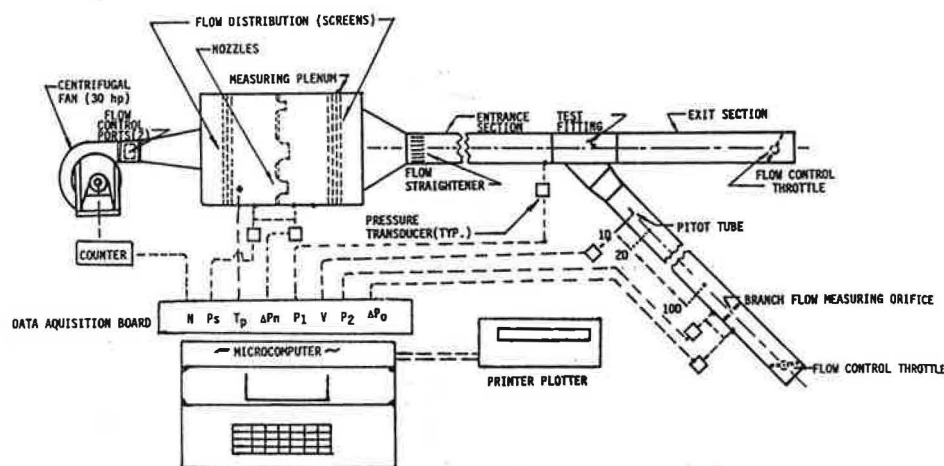
Air flow through the duct system was provided by a centrifugal fan driven by a 30-hp motor. Flow rates were determined from measurements of pressure drop across a set of spun aluminum, longradius, ASME-type nozzles mounted within a plenum. Figure 1 is a schematic of the system, configured for tests with branch-type fittings. A sheet metal transition connected the fan outlet to the plenum inlet. Air was dumped from ports on both sides of the transition between the fan and plenum to control flow rate. A 24 to 14/10-in.-diameter transition was used between the plenum and an entrance length of 14- or 10-in.-diameter duct. A second transition was used between the entrance section and the test system duct. A flow straightener, fabricated in accordance with ASHRAE Standard 51-1985 (ASHRAE 1985a), was placed in one section of the upstream 14- or 10-in.-diameter duct. A sufficient length of test system duct was placed upstream of the fitting to provide fully developed flow at the fitting entrance. The length was greater in all cases than that calculated by

$$Le/D \approx 4.4 Re^{1/2} \quad (1)$$

Equation 1 is given by White (1986) to estimate the length required for turbulent flow to develop.

Nozzles having nominal diameters of 4, 6, and 8 inches were used in determining the supply flow rate. An orifice plate, calibrated against the nozzles, was used to

E.I. Griggs and W.B. Swim are Professors and H.G. Yoon is a Graduate Assistant in the Department of Mechanical Engineering, Tennessee Technological University, Cookeville.



Dimensions for FIG. 1 are: 42 wide by 200 deep.

Figure 1 Schematic of experimental system, configured for tests with a branch-type fitting

determine flow rate in the branch. During testing, a particular nozzle or combination of nozzles was used in establishing a desired flow rate. Unused nozzles were plugged with smooth vinyl balls.

An apparatus was built to facilitate systematic positioning of pitot tubes. The apparatus consisted principally of a structural base, a movable traversing fixture, and items to aid in automated measurements. The base was supported on casters that allowed it to be positioned in proper alignment with the duct and test fitting. Extended braces and straps permitted a 16-ft section of duct to be properly aligned and firmly attached to the base. The traversing fixture supported two pitot tubes and was designed to move one along a horizontal line of travel and the other along a vertical line of travel. Computer-controlled stepping motors were used to move the pitot tubes across the duct. The traversing fixture was mounted on guide rods running along the top of the apparatus. A computer-controlled chain drive was used to position the fixture longitudinally.

Ambient dry- and wet-bulb temperatures and barometric pressures were measured to determine ambient air density, which was corrected for other stations within the test system using local pressure and temperature measurements. Pressure drop across the ASME nozzle bank and upstream static pressure were measured to determine supply flow rate. When branch ducts were involved, the pressure drop across the orifice and upstream static pressure were measured to determine branch flow rate. Pressure differentials were obtained using micromanometers having a scale readability of 0.001 in. H₂O.

The pressure differential output of each pitot tube was routed to a capacitance-type pressure transducer, which, in turn, produced an output voltage that was routed directly to the data acquisition system. The data acquisition system was calibrated and checked routinely against a reference micromanometer. Pitot tube outputs were processed

automatically. The fitting and upstream duct were leak checked prior to making velocity measurements.

SCOPE OF TESTS

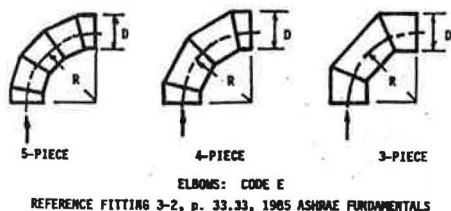
Each fitting is coded first by a letter or set of letters designating the fitting. This was followed by a sequential number assigned to the fitting in its category. The next digit was always the letter D followed by a number indicating target average test velocities. For elbows, contractions, and diffusers, D1, D2, and D3 represent, respectively, target velocities of 1000, 1750, and 2500 fpm. For wyes and tees, a two-digit number after D indicates a particular combination of main and branch target velocities, with 1, 2, and 3 associated, respectively, with 1000, 1750, and 2500 fpm. Two examples follow.

E2D2	...	E	2	D2	
.	Target Velocity After Fitting = 1750 fpm
.	Elbow Number 2
.	Designates Elbow
DY1D12	...	DY	1	D12	
.	Target Velocities After Fitting
.	1000 fpm (main)
.	1750 fpm (branch)
.	Wye Number 1 for DY group
.	Wyes of particular type

TABLE 1
Identification of Elbows Tested

Code	Dia. (inches)	R/D	Number of Pieces	Turning Angle (degrees)	Average Velocity (sfpm)		
					Case D1	Case D2	Case D3
E1	6	1.0	3	90	994	1629*	2277
E2	6	1.0	4	90	991	1612*	2238
E3	6	1.0	5	90	1020	1656*	2278
E4	6	1.5	3	90	960	1611*	2213
E5	6	1.5	4	90	946	1609*	2311
E6	6	1.5	5	90	951	1618*	2284
E7	10	1.0	3	90	993	1634*	2340
E8	10	1.0	4	90	988	1675*	2368
E9	10	1.0	5	90	988	1684*	2369
E10	10	1.5	3	90	981	1632*	2362
E11	10	1.5	4	90	961	1651*	2340
E12	10	1.5	5	90	965	1641*	2350
E13	16	1.0	3	90	940	1630*	2354
E14	16	1.0	4	90	980	1644*	2344
E15	16	1.0	5	90	932	1653*	2354
E16	16	1.5	3	90	978	1644*	2370
E17	16	1.5	4	90	979	1648*	2348
E18	16	1.5	5	90	978	1639*	2347
E19	6	1.0	3	45	959	1647*	2301
E20	6	1.0	4	45	951	1671*	2299
E21	6	1.0	5	45	947	1660*	2295
E22	6	1.5	3	45	945	1679*	2333
E23	6	1.5	4	45	946	1672*	2345
E24	6	1.5	5	45	947	1676*	2333
E25	10	1.0	3	45	938	1690*	2362
E26	10	1.0	4	45	973	1626*	2358
E27	10	1.0	5	45	981	1641*	2356
E28	10	1.5	3	45	974	1640*	2358
E29	10	1.5	4	45	904	1636*	2342
E30	10	1.5	5	45	986	1637*	2373
E31	16	1.0	3	45	924	1647*	2345
E32	16	1.0	4	45	911	1635*	2334
E33	16	1.0	5	45	928	1636*	2363
E34	16	1.5	3	45	920	1642*	2375
E35	16	1.5	4	45	926	1641*	2346
E36	16	1.5	5	45	930	1637*	2344

*Designates cases for which complete profiles were obtained.



Tables 1 through 5 identify the 69 fittings. Average velocities for the tests are given in sfpm. Since air density within the duct was typically less than standard density, velocities in sfpm are smaller than actual target velocities of 1000, 1750, and 2500 fpm. Cases denoted by an asterisk (*) in Tables 1 through 5 are those for which vertical and horizontal traverses were made. Only centerline velocities were measured for the other cases.

RESULTS

The final report (Griggs et al. 1987) documents the extensive results. Illustrative centerline velocity data plots, velocity profiles, and summaries are included in this paper.

Centerline velocity data for all elbows are given in Table 6. Results for all elbows are similar, with the most

apparent distinction being between those for 45° and 90° elbows. Centerline velocities for contractions and diffusers are given in Tables 7 and 8. Marked distinction was found in the profiles downstream of these fittings when operating as a diffuser and when operating as a contraction. Centerline velocities for round-to-round diverging junctions are given in Table 9. Table 10 contains centerline data for round diverging wyes having a 45° elbow tap connection. Centerline data for junctions with a rectangular main and a 6-in.-diameter branch are listed in Table 11.

The centerline velocity data were examined while considering the physical distinction between fittings within a category to see if variation in data could be correlated with particular factors. The most discernible influence was angle for elbows, wyes, and tees.

Groupings of data were plotted to portray the spread in centerline velocities at each longitudinal measuring station. The solid line in each plot connects the average values at each position. Elbow data are shown in Figure 2. Conical contraction and conical diffuser data are plotted in Figure 3. All data for contractions are plotted together, while those for diffusers have been grouped for each of the three diffusion angles. Note the scale difference between plots for contractions and diffusers when comparing results. Figure 4 is for round-to-round junctions, while Figure 5 is for rectangular-to-round junctions.

The spread in centerline data was large immediately after the fitting in all cases. The most consistent consolidation of data at the 10-diameter station was noted for the elbows. The dispersion of data at all stations was more pronounced for the wyes and tees. Data spread in general suggests situational dependence, but attempts to identify such through examination of data sorted by distinctive elements within a category were unfruitful. Consequently, it is recommended that tabulated data be used without attempting to rely on a single number within a category.

The distinction between vertical and horizontal profiles and downstream profile evolution is shown for representative tests in Figures 6 through 13. The broken line in each case shows where V/V_0 is unity. The scale permits qualitative evaluation at best, but all data represented here and all other profile data can be examined more quantitatively by referring to expanded plots given in the project report (Griggs et al. 1987). A few additional tests were included where measurements were made farther from the fitting than the upper value of 10 diameters included in the original work, with the intent being to explore the continuing effect of flow development, which did not occur at the 10-diameter location in all cases. Figures 12 and 13 show profiles for these additional tests.

Velocity profiles exhibited some interesting patterns. The vertical profiles following elbows exhibited considerable symmetry, while asymmetry was evident in the horizontal ones near the fitting (Figures 6 and 12). For contractions, the velocity profiles were similar and nearly symmetrical for both the vertical and horizontal traverses. The similarity and symmetry also occurred for diffusers, but the patterns and local velocity magnitudes were quite distinct for the two different fittings. Example cases for wyes and tees are shown in Figures 9, 10, 11, and 13. Vertical profiles for wyes and tees were also more consistently symmetrical than were horizontal profiles. Within the range of conditions

examined for each fitting type, larger variations in patterns occurred for junctions than for the undivided fittings (elbows, contractions, and diffusers). The absence of symmetry and the fact that larger velocity gradients were present close to the fitting undoubtedly contributed to the spread in measured centerline velocities noted earlier.

MEASUREMENT UNCERTAINTIES

Uncertainty in the results, reported as \bar{V}/\bar{V} , is due to uncertainties in local velocity, flow rate, and cross-sectional area determinations. Pressure differentials from the pitot tubes were routed to a capacitance-type transducer, whose output was, in turn, routed to a computer-aided data acquisition system. The complete system was routinely calibrated against a micromanometer having a scale readability of 0.001 in. H_2O . Routine experience with these units indicates that this accuracy is difficult to ascertain through extensive production-type testing. An uncertainty in pressure differential measurement of ± 0.001 in. H_2O would correspond to a possible error ranging from $\pm 0.26\%$ to $\pm 1.6\%$ for the range of velocities encountered in this work. With a more realistic uncertainty of ± 0.003 in. H_2O , the resultant range would be $\pm 0.8\%$ to $\pm 4.8\%$. The larger percentages are for velocities of about 1000 fpm.

A detailed error analysis, made for the flow-measuring system used in this work, was previously reported to ASHRAE (Henderson et al. 1986). Error estimates included therein depended on flow conditions, but they indicated that flow rate should be within $\pm 2\%$ when care is exercised throughout. Swim (1986) has also discussed practical problems associated with flow rate measurement and use of pitot tubes. For \bar{V}/\bar{V} values near 1.0, an error of $\pm 3\%$ indicates a band on the ratio of about ± 0.03 . Some of the data resulted in a smaller spread than this, but accuracy better than $\pm 3\%$ would be most difficult to claim.

FLOW RATE ESTIMATION

Determining flow rate from velocity measurement probably ranges in practice from making a single measurement (e.g., centerline) to detailed traversing. Estimating flow rate from centerline velocity is rooted in the validity of this approach for symmetrical, fully developed flow. When fully developed flow in a circular passage can be represented by the power law expression,

$$V = V_c [1 - (2r/D)]^{1/n} \quad (2)$$

the relationship between average and centerline velocities is

$$\bar{V}/V_c = \frac{2n^2}{(n+1)(2n+1)} \quad (3)$$

The power law exponent varies with Reynolds number (Sissom and Pitts 1972). When flows prevail where velocities are not governed by known mathematical relationships, the use of only the single centerline velocity could lead to considerable error unless its relationship to the average velocity is known from experimental work. The extensive tabulations of centerline velocity provided by this study should be useful for the range of conditions covered and should provide insight for other cases as well.

HVAC testing and balancing practitioners most likely make multiple velocity measurements when determining flow rate. Detailed specifications for making traverses are specified in a SMACNA manual (SMACNA 1983) and in Chapter 13 of the 1985 ASHRAE Fundamentals (ASHRAE 1985b). Selected sets of data from this work were used to estimate flow rate by interpolating data to obtain velocities at radii specified in ASHRAE (1985b).

The scheme used in averaging velocities for flow rate estimation was based on the traverse pattern specified in Chapter 13 of ASHRAE (1985b). The specification requires measurement of 20 velocities at prescribed radii. Ten are made on one diameter and the other ten on a second diameter 90° from the first. Flow rate calculations were made via this technique for 20 sets of data, encompassing data from fittings of each category included in this work. Estimated flow rates, expressed as an average of \bar{V}/\bar{V} , are tabulated in Tables 12 through 15. A value of 1.0 would indicate exact prediction. For each case, results are given for the horizontal and vertical traverse data at each of the five longitudinal measuring stations. The ratio corresponding to the prescribed 20-point averaging scheme is given by the average of two tabular entries. The reason that separate numbers are shown for vertical and horizontal is to indicate what is obtained if only one traverse is made in the respective plane. The ratios shown for each direction are what is obtained if only 10 values, based on a single traverse, are used assuming symmetry in the other plane. When averaging the ratios for both directions, consistent with the two-diameter traverse, the error is less than the maximum error based on a single traverse in all cases. In several cases where large error occurs if only one plane is used, the two-plane error is small because the error for the two single-plane traverses counteracts. Individual data spread for each case examined is best obtained from Tables 12 through 15. An abridged summary follows.

For each fitting category, two numbers are shown. One is the maximum error calculated for the selected cases using only a single traverse. The other, in parentheses, is the maximum error for each category for the cases examined if two traverses are used. These are listed to provide an overview. Since variations occurred for different fittings within a category, more specific case-by-case details should be obtained from Tables 12 through 15. The largest errors occurred for data obtained nearest the fitting.

More consistent results for all cases are obtained when flow rate determinations are based on measurements 10 diameters downstream of the fitting. When measurements must be made closer to a fitting, careful scrutiny should be given to interpretation. The data obtained in this work and included here should provide both qualitative and quantitative insight to those who make field velocity measurements downstream of HVAC sheet metal fittings.

APPLICATION TO THE LOCATION OF VELOCITY/VELOCITY PRESSURE SENSORS

The data gathered in this study are intended to be of practical use in the determination of the optimal location of velocity/velocity pressure sensors. Tables 6 through 11 present a ratio of centerline velocity to average duct velocity.

	1D	2D	4D	6D	10D
1. Elbows	16.4 (5.2)	10.0 (6.8)	6.8 (6.2)	6.2 (5.7)	4.9 (3.9)
2. Contractions	2.9 (2.1)	2.9 (2.2)	3.6 (3.0)	4.6 (3.8)	4.2 (3.1)
3. Diffusers	40.6 (35.3)	27.7 (24.7)	11.5 (11.8)	5.3 (4.8)	1.2 (1.1)
4. Y's(*)	44.7 (16.8)	22.6 (5.8)	12 (5.9)	10.5 (6.2)	7.1 (5.4)
5. DY's(*)	18.7 (8.4)	15.4 (9.1)	11.7 (8.3)	10.4 (8.1)	8.1 (6.5)
6. T's(*)	25.8 (10.5)	20.5 (4.0)	6.4 (4.0)	5.1 (2.7)	2.9 (2.6)

*See Nomenclature

by for various fitting types, traverse locations, and main/branch velocities. These data can be used to:

1. determine the distance between the fitting and the sensor that is required to obtain a centerline velocity representative of average duct velocity,
2. determine the distance between a fitting and velocity sensor required to obtain a repeatable ratio of centerline velocity to average duct velocity over a range of average duct velocities that would be similar to the range of velocities experienced in a VAV system,
3. develop a recommendation of certain fittings that should be avoided in designing VAV systems due to their inherent tendency to disrupt the flow leading into a VAV control unit.

The remainder of this section evaluates the tested fittings with these objectives in mind.

Table 6 presents the ratios of centerline to average duct velocity for varying sizes of 90° elbows of 3-, 4-, and 5-piece construction at various average duct velocities. For almost all elbows tested, a distance of 6 diameters of straight duct between the elbow and the sensor is required to obtain a centerline velocity representative of the average duct velocity. However, the repeatability of the ratio of the centerline to average velocity at various duct velocities is evident at two diameters of distance. Placement of a velocity sensor at this location should yield repeatable measurements that all have the same ratio to average duct velocity. Utilization of the sensor in such a location would simply involve a correction to the sensor calibration curve based on the ratio of centerline to average duct velocity for the installed sensor.

Tables 7 and 8 present similar data for round-to-round contraction and diffusion fittings. Measurements taken as far as 10 diameters from the fittings failed to identify a location where the centerline velocity was representative of the average duct velocity. However, when the fittings were subjected to various duct velocities, these ratios were basically repeatable at distances as little as one diameter between the fitting and the measurement location.

Table 9 presents data for round diverging junctions. Fittings Y1, Y2, and Y3 represent junctions where the branch tap exits at 90° from the main duct. These fittings demonstrated a centerline velocity that was relatively representative of average duct velocity at a measurement location four diameters from the fitting. For all locations less than four diameters, neither a representative nor repeatable measurement was indicated. Fittings Y4, Y5, and Y6 represent fittings whose branch tap exits at 30° from the main duct. These fittings exhibited no measurement loca-

tion less than 10 diameters downstream where either the centerline velocity was representative of the average duct velocity or the ratio of the two velocities was consistent. As a result, these fittings should be avoided when designing VAV systems.

Table 10 contains similar data for round diverging wyes with a 45° elbow tap connection. Again, no location within 10 diameters of the fitting was determined where either the centerline velocity was indicative of the average duct velocity or their ratios were repeatable over the prescribed range of velocities. These fittings should also be avoided when designing VAV duct systems.

Table 11 represents data for diverging junctions with a rectangular main duct feeding a round tap. Fittings T1, T2, and T3 are fittings with the branch tap exiting at a 30° angle from the main duct. The centerline velocity was not representative of the average duct velocity at any measurement location within 10 diameters of the fitting. The ratio of the centerline to average velocity was fairly repeatable at distances 6 to 10 diameters from the fitting. These distances are not, however, very practical in actual installations. Fittings T4, T5, and T6 are fittings where the branch tap exits at 90° from the main duct. Again, no measurement location was identified within 10 diameters of the fitting where the centerline velocity was indicative of the average velocity. Fairly consistent ratios of centerline to average velocity were obtained at distances of four diameters and greater from the fitting. Fittings T7, T8, and T9 are identical to T1, T2, and T3 except that they have a conical branch connection to the main duct. This difference in construction makes no significant improvement in performance. Fittings T10, T11, and T12 are identical to T4, T5, and T6 except that they also contain a conical branch tap. Again, no significant improvement in performance was noted.

SUMMARY OF GUIDELINES FOR SENSOR LOCATION

Centerline velocity measurements taken downstream of elbows can be expected to yield reasonable accuracy provided the measurement location is separated from the fitting by at least 6 diameters of straight, rigid duct downstream of the elbow. Similar measurements taken in a round, rigid branch duct exiting at a right angle from a rectangular main and a round, diverging junction with the branch exiting at 90° from the main duct can be expected to yield accurate results provided the sensor location is separated by at least 4 diameters of straight, rigid duct from the main duct. Other fittings tested did not exhibit any location within 10 diameters of the fitting where the centerline velocity was indicative of the average duct velocity.

Measurements made following rigid 90° elbows and round-to-round contracting and diffusing fittings indicated that a consistent ratio of centerline to average velocity (V_c/V) is obtainable with as little as 2 diameters of rigid duct between the fitting and measurement location. Consistency of this ratio is also obtainable when 4 diameters of straight duct separate the sensor and a round diverging junction with a branch exit angle of 90°. Diverging junctions with rectangular mains and a round branch exiting at 30° require 6 to 10 diameters separation for a consistent ratio of V_c/V to exist, and 4 diameters when the branch exits at a right angle rather than 30°.

In actual field application, the lengths of straight, rigid duct noted above are seldom available upstream of desired sensor locations. All of these facts lead to one simple conclusion—once installed, the velocity sensor should be calibrated by means of determining the branch air flow by traverse or outlet readings and establishing a sensor calibration curve that relates to the installed device. Care should be taken to provide as much straight duct immediately preceding the sensor as possible. Fittings identified as poor for use preceding such sensors should be avoided. Field measurement—and thus control—accuracies should not be expected to exceed or even equal those obtained in the laboratory setup of this study. Data are not applicable to flexible duct connections from the duct main to a terminal box.

CONCLUSIONS

Within the scope of tests made in this project, the following conclusions are offered.

1. At 10 diameters after fittings, flow is not completely symmetrical or fully developed. Lack of development appears more prevalent for divided fittings than undivided ones. Data obtained for three additional tests at larger distances show near development at approximately 25 diameters, but even for such extended lengths, exact coincidence of vertical and horizontal profiles is not observed.
2. V_c/V for elbows is not markedly influenced by flow rate, diameter, number of segments, or R/D . Turning angle appears to have the most distinctive influence on results. Vertical profiles exhibit near symmetry, but horizontal ones are asymmetric.
3. Most symmetry occurs for conical contractions. Profiles are flat immediately after the fitting; they appear almost developed at 10 diameters downstream. Magnitudes of V_c/V varied with contraction angle.
4. Pronounced jetting occurs immediately after conical diffusers with separation occurring near the wall. Velocity profiles are markedly different from those after conical contractions. Magnitudes of V_c/V depended strongly on diffusion angle.
5. For round-to-round and rectangular-to-round junctions, the main-to-branch angle and the ratio of main-to-branch flow rate appears to influence velocity magnitudes and profile patterns. For these divided flow fittings, downstream vertical profiles exhibit near symmetry, as is the case with elbows, but horizontal profiles are characterized by marked asymmetry.
6. Use of single-plane traverses immediately after fittings

(e.g., up to 4 diameters) for flow rate determination can lead to large error. More reliable determinations (e.g., on the order of $\pm 5\%$) can be made if the proper traverses are made at distances greater than 10 diameters.

7. Placement of a single-point velocity sensor at least two diameters downstream of elbows will provide repeatable measurements; it would be necessary to calibrate the sensor using data for the ratios of measured centerline to average velocities.

ACKNOWLEDGMENTS

The work reported in this paper was funded under ASHRAE 403RP. The guidance and aid provided by TC 9.7 were most helpful and sincerely appreciated.

NOMENCLATURE

D	= duct diameter (in.)
fpm	= feet per minute
L_a	= entrance length
n	= exponent in power law equation (Equation 2)
r	= variable radius within flow (Equation 2)
R	= centerline radius of elbows or radius of round duct (in.)
Re_D	= Reynolds number (dimensionless)
sfp	= standard feet per minute
V	= local velocity (fpm)
V_c	= centerline velocity (fpm)
\bar{V}	= mass-average velocity (fpm or sfp)

Fitting Code Prefixes

C	= prefix used in coding contractions
DC	= prefix used in coding diffusers
DY	= prefix used in coding round-to-round wyes with a 45° elbow connecting main to branch
E	= prefix used in coding elbows
T	= prefix used in coding rectangular-to-round junctions
Y	= prefix used in coding round-to-round junctions

REFERENCES

- ASHRAE. 1985a. ASHRAE Standard 51-1985, "Laboratory methods of testing fans for rating." Atlanta: American Society of Heating, Refrigerating, and Air-Conditioning Engineers, Inc.
- ASHRAE. 1985b. *ASHRAE handbook—1985 fundamentals*, chapters 13 and 33. Atlanta: American Society of Heating, Refrigerating, and Air-Conditioning Engineers, Inc.
- Griggs, E.I.; Swim, W.B.; and Yoon, H.G. 1987. "Proper placement of air control sensors." ASHRAE 403-RP, Phase II Final Report (Parts I-VI), December 31. Cookeville: Tennessee Technological University.
- Henderson, G.H.; Griggs, E.I.; and Swim, W.B. 1986. "Experimental determination of friction pressure losses in modern day HVAC ducts." Final Report—Part II, ASHRAE 383-RP, January. Cookeville: Tennessee Technological University.
- Sissom, L.E., and Pitts, D.R. 1972. *Elements of transport phenomena*. New York: McGraw-Hill.
- SMACNA. 1983. *HVAC system testing, adjusting and balancing*, pp. 5.2-5.7. Vienna, VA: Sheet Metal and Air Conditioning Contractors' National Association, Inc.
- Swim, W.B. 1986. "Laboratory testing of air ducts and fittings to determine flow resistance." *Proceedings of Air Movement and Distribution Conference*, May 27-29, Purdue University, West Lafayette, IN.
- White, F.M. 1986. *Fluid mechanics*. New York: McGraw-Hill.

TABLE 2
Identification of Round-to-Round Diverging (Diffusers)
and Converging (Contractions) Fittings Tested

Code No.	Inlet Dia. to Outlet Dia. (in.)	Divergence Angle (deg.)	Average Velocity (sfpm)			
			D1	D2	D3	D4
DCD1	6 to 10	20	964	1584*	2448	590*
DCD2	6 to 10	45	956	1659*	2260	600*
DCD3	6 to 10	90	971	1672*	2228	602*
DCD4	6 to 12	20	904	1598*	2369	403*
DCD5	6 to 12	45	927	1597*	2166	396*
DCD6	6 to 12	90	930	1602*	2117	399*
CD1	10 to 6	20	996*	1573*	2337	4394*
CD2	10 to 6	45	1028	1587*	2368	4460*
CD3	10 to 6	90	1011	1563*	2339	4405*
CD4	12 to 6	20	994*	1650*	2415	6402*
CD5	12 to 6	45	898	1500*	2436	6256*
CD6	12 to 6	90	924	1587*	2303	6351*

*Designates cases for which complete profiles were obtained.

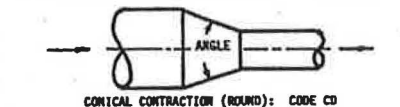
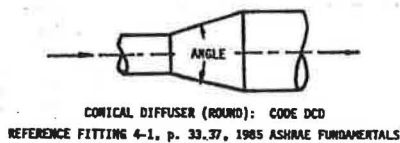


TABLE 3
Identification of Round-to-Round Wyes Tested

Code No.	Diameter of Main (inches)	Diameter of Branch (inches)	Divergence Angle (degrees)	V Branch								
				V Main								
				D11	D12	D13	D21	Test D22	D23	D31	D32	D33
Y1	10	6	90	982	952	927	1611	1604*	1590	2281	2305	2280
				928	1648	2281	935	1614	2270	935	1623	2285
Y2	12	6	90	933	933	922	1618*	1610*	1580*	2257	2278	2295
				933	1631	2268	936	1617	2281	932	1658	2271
Y3	16	6	90	909	882	946	1592	1591*	1572	2267	2284	2308
				936	1623	2265	934	1612	2267	935	1620	2252
Y4	10	6	30	908	924	900	1621	1610*	1631	2323	2293	2298
				928	1658	2259	946	1641	2285	935	1632	2264
Y5	12	6	30	913	912	928	1604*	1620*	1621*	2285	2278	2297
				935	1610	2255	939	1623	2273	928	1618	2266
Y6	16	6	30	957	942	905	1612	1629*	1605	2329	2280	2305
				937	1619	2258	927	1610	2283	931	1622	2289

*Designates cases for which complete profiles were obtained.

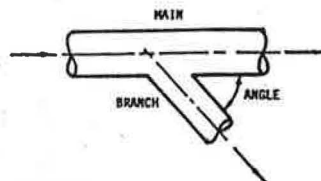


TABLE 4
Identification of Tested Wyes with 45° Elbow-to-Branch Connection

Code No.	Inlet Diameter (inches)	Outlet Diameter (inches)	Branch Diameter (inches)	V Branch								
				V Main								
				D11	D12	D13	D21	Test D22	D23	D31	D32	D33
DY1	10	6	6	945	981	931	1619	1589*	1586	2290	2261	2270
				938	1635	2264	942	1620	2283	924	1636	2250
DY2	12	6	6	921	920	947	1610*	1617*	1629*	2318	2304	2300
				935	1637	2267	933	1634	2271	932	1631	2270
DY3	16	6	6	906	891	924	1622	1659*	1623	1646	1728	1811
				938	1622	2268	939	1631	2283	924	1623	2266

*Designates cases for which complete profiles were obtained.

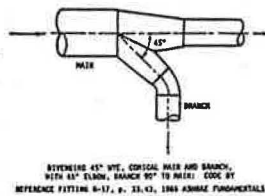


TABLE 5
Identification of Tested Tees with a Rectangular Main and a 6-Inch Diameter Branch

Code No.	Main Width by Height (inches)	Branch Angle (degrees)	Tap Type	V Branch									
				V Main					Test				
				D11	D12	D13	D21	D22	D23	D31	D32	D33	
T1	8 x 7	30	1	923	913		1618	1638*	1602	2272	2270	2280	
				931	1642		924	1617	2268	935	1619	2262	
T2	12 x 10	30	1	904	898	899	1605*	1600*	1592*	2262	2263	2253	
				935	1615	2234	931	1613	2277	935	1630	2265	
T3	18 x 10	30	1	939	923	908	1596	1596*	1592	2284	2288	2277	
				935	1600	2245	933	1619	2265	923	1522	2256	
T4	8 x 7	90	1	912	910		1630	1596*	1608	2265	2272	2293	
				933	1602		931	1629	2270	933	1634	2268	
T5	12 x 10	90	1	934	931	921	1591*	1577*	1572*	2252	2253	2244	
				933	1632	2264	928	1621	2265	932	1631	2268	
T6	18 x 10	90	1	954	953	957	1623	1584*	1612	2281	2277	2281	
				937	1602	2264	935	1594	2265	934	1595	2262	
T7	8 x 7	30	2	910	929		1596	1602*	1550	2269	2281	2285	
				937	1661		935	1614	2265	935	1628	2269	
T8	12 x 10	30	2	942	934	914	1590*	1584*	1588*	2269	2265	2259	
				933	1620	2270	928	1603	2265	931	1622	2265	
T9	18 x 10	30	2	917	925	935	1588	1584*	1590	2303	2296	2295	
				935	1595	2256	942	1602	2262	935	1600	2271	
T10	8 x 7	90	2	910	934		1610	1600*	1651	2303	2311	2279	
				933	1659		935	1621	2261	931	1628	2254	
T11	12 x 10	90	2	904	906	904	1579*	1593*	1591*	2223	2214	2188	
				935	1635	2257	935	1628	2269	939	1640	2263	
T12	18 x 10	90	2	899	899	912	1608	1599*	1605	2286	2278	2278	
				934	1601	2259	923	1598	2261	939	1591	2264	

*Designates causes for which complete profiles were obtained.
(1) Butt (Round) Connection; (2) Conical Connection

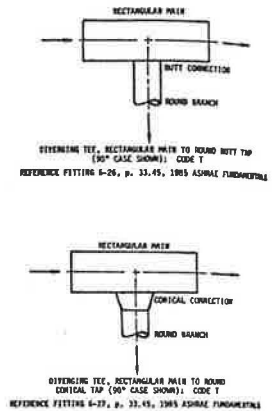


TABLE 6
Centerline Velocity Data for Elbows

Code	Dia.No. (in.Fcm.)	R/D	Angle (Deg.)	Velocity Ratio, V_o / V_{avg} .					
				1D	2D	4D	6D	10D	
E1D1	6	3	1	90	0.72	0.77	0.92	1.03	1.11
E1D2	6	3	1	90	0.73	0.77	0.92	1.02	1.08
E1D3	6	3	1	90	0.75	0.79	0.94	1.03	1.10
E2D1	6	4	1	90	0.76	0.78	0.94	1.04	1.11
E2D2	6	4	1	90	0.81	0.80	0.94	1.03	1.10
E2D3	6	4	1	90	0.83	0.81	0.94	1.04	1.11
E3D1	6	5	1	90	0.71	0.79	0.96	1.06	1.11
E3D2	6	5	1	90	0.75	0.81	0.98	1.07	1.12
E3D3	6	5	1	90	0.76	0.81	0.96	1.06	1.11
E4D1	6	3	1.5	90	0.73	0.75	0.92	1.01	1.08
E4D2	6	3	1.5	90	0.74	0.76	0.94	1.02	1.08
E4D3	6	3	1.5	90	0.79	0.77	0.94	1.02	1.08
E5D1	6	4	1.5	90	0.77	0.79	0.95	1.03	1.07
E5D2	6	4	1.5	90	0.76	0.79	0.96	1.03	1.08
E5D3	6	4	1.5	90	0.77	0.79	0.95	1.03	1.08
E6D1	6	5	1.5	90	0.69	0.79	0.96	1.03	1.08
E6D2	6	5	1.5	90	0.68	0.80	0.98	1.05	1.09
E6D3	6	5	1.5	90	0.72	0.80	0.98	1.05	1.09
E7D1	10	3	1	90	0.79	0.77	0.92	1.01	1.08
E7D2	10	3	1	90	0.83	0.77	0.92	1.02	1.09
E7D3	10	3	1	90	0.88	0.79	0.91	1.01	1.08
E8D1	10	4	1	90	0.79	0.78	0.95	1.05	1.11
E8D2	10	4	1	90	0.84	0.81	0.95	1.04	1.10
E8D3	10	4	1	90	0.83	0.80	0.95	1.04	1.10
E9D1	10	5	1	90	0.86	0.79	0.95	1.04	1.12
E9D2	10	5	1	90	0.87	0.81	0.95	1.05	1.11
E9D3	10	5	1	90	0.90	0.82	0.96	1.04	1.10
E10D1	10	3	1.5	90	0.76	0.76	0.93	1.01	1.06
E10D2	10	3	1.5	90	0.77	0.77	0.94	1.01	1.07
E10D3	10	3	1.5	90	0.82	0.77	0.93	1.00	1.07
E11D1	10	4	1.5	90	0.64	0.83	0.99	1.04	1.08
E11D2	10	4	1.5	90	0.69	0.81	0.98	1.04	1.08
E11D3	10	4	1.5	90	0.70	0.83	0.99	1.05	1.09
E12D1	10	5	1.5	90	0.72	0.82	0.99	1.05	1.09
E12D2	10	5	1.5	90	0.74	0.82	0.98	1.05	1.08
E12D3	10	5	1.5	90	0.79	0.84	1.00	1.06	1.09
E13D1	16	3	1	90	0.81	0.77	0.94	0.96	1.09
E13D2	16	3	1	90	0.84	0.79	0.94	1.03	1.09
E13D3	16	3	1	90	0.85	0.79	0.95	1.03	1.09
E14D1	16	4	1	90	0.85	0.80	0.95	1.03	1.09
E14D2	16	4	1	90	0.90	0.80	0.95	1.01	1.09
E14D3	16	4	1	90	0.93	0.81	0.95	1.03	1.09
E15D1	16	5	1	90	0.82	0.83	0.98	1.05	1.10
E15D2	16	5	1	90	0.88	0.84	0.96	1.04	1.10
E15D3	16	5	1	90	0.87	0.82	0.97	1.04	1.10

TABLE 6
Centerline Velocity Data for Elbows (Continued)

Code	Dia. No. (in. Pos.)	R/D	Angle (deg.)	Velocity Ratio, $V_c / V_{avg.}$			
				1D	2D	4D	10D
E14D1	14	3	1.5	90	0.87	0.81	0.92
E14D2	14	3	1.5	90	0.91	0.80	0.92
E14D3	14	3	1.5	90	0.91	0.80	0.91
E17D1	16	4	1.5	90	0.80	0.83	0.97
E17D2	16	4	1.5	90	0.80	0.83	0.97
E17D3	16	4	1.5	90	0.81	0.82	0.96
E17D4	16	4	1.5	90	0.76	0.85	1.00
E18D1	16	5	1.5	90	0.82	0.85	0.99
E18D2	16	5	1.5	90	0.82	0.85	0.99
E18D3	16	5	1.5	90	0.84	0.85	1.00
E19D1	6	3	1	45	1.23	0.93	0.98
E19D2	6	3	1	45	1.21	0.89	0.93
E19D3	6	3	1	45	1.25	0.96	0.94
E20D1	6	4	1	45	1.20	0.83	0.87
E20D2	6	4	1	45	1.22	0.86	0.89
E20D3	6	4	1	45	1.24	0.90	0.90
E21D1	6	5	1	45	1.19	0.86	0.89
E21D2	6	5	1	45	1.18	0.88	0.92
E21D3	6	5	1	45	1.23	0.90	0.92
E22D1	6	3	1.5	45	1.17	0.88	0.88
E22D2	6	3	1.5	45	1.17	0.89	0.91
E22D3	6	3	1.5	45	1.20	0.92	0.91
E23D1	6	4	1.5	45	1.21	0.83	0.89
E23D2	6	4	1.5	45	1.21	0.85	0.91
E23D3	6	4	1.5	45	1.22	0.88	0.89
E24D1	6	5	1.5	45	1.21	0.86	0.90
E24D2	6	5	1.5	45	1.22	0.87	0.92
E24D3	6	5	1.5	45	1.23	0.92	0.92
E25D1	10	3	1	45	1.19	0.84	0.86
E25D2	10	3	1	45	1.21	0.87	0.89
E25D3	10	3	1	45	1.24	0.92	0.90
E26D1	10	4	1	45	1.22	0.88	0.87
E26D2	10	4	1	45	1.24	0.91	0.89
E26D3	10	4	1	45	1.25	0.95	0.91
E27D1	10	5	1	45	1.20	0.84	0.86
E27D2	10	5	1	45	1.22	0.87	0.87
E27D3	10	5	1	45	1.24	0.90	0.90
E28D1	10	3	1.5	45	1.20	0.90	0.87
E28D2	10	3	1.5	45	1.21	0.93	0.87
E28D3	10	3	1.5	45	1.22	0.95	0.89
E29D1	10	4	1.5	45	1.19	0.88	0.85
E29D2	10	4	1.5	45	1.21	0.92	0.88
E29D3	10	4	1.5	45	1.22	0.95	0.90
E30D1	10	5	1.5	45	1.19	0.87	0.87
E30D2	10	5	1.5	45	1.19	0.91	0.87
E30D3	10	5	1.5	45	1.21	0.93	0.86



TABLE 6
Centerline Velocity Data for Elbows (Concluded)

Code	Dia. No. (in. Pos.)	R/D	Angle (deg.)	Velocity Ratio, $V_c / V_{avg.}$			
				1D	2D	4D	10D
E31D1	16	3	1	45	1.22	0.97	0.89
E31D2	16	3	1	45	1.22	0.98	0.91
E31D3	16	3	1	45	1.23	1.00	0.90
E32D1	16	4	1	45	1.24	0.95	0.90
E32D2	16	4	1	45	1.24	1.00	0.91
E32D3	16	4	1	45	1.25	1.02	0.93
E33D1	16	5	1	45	1.22	0.96	0.90
E33D2	16	5	1	45	1.24	0.98	0.90
E33D3	16	5	1	45	1.25	1.01	0.93
E34D1	16	3	1.5	45	1.21	1.01	0.88
E34D2	16	3	1.5	45	1.20	1.05	0.88
E34D3	16	3	1.5	45	1.20	1.05	0.88
E35D1	16	4	1.5	45	1.20	0.99	0.87
E35D2	16	4	1.5	45	1.20	1.04	0.88
E35D3	16	4	1.5	45	1.20	1.05	0.88
E36D1	16	5	1.5	45	1.19	1.00	0.87
E36D2	16	5	1.5	45	1.20	1.04	0.88
E36D3	16	5	1.5	45	1.20	1.07	0.88

TABLE 7
Centerline Velocity Data for Round-to-Round Contractions

Code	Inlet Dia. to Outlet Di Angle (in.) (Deg.)			Velocity Ratio, V_c / V_{avg}				
				1D	2D	4D	6D	10D
CD1D1	10 TO 6	20		1.08	1.09	1.10	1.13	1.15
CD1D2	10 TO 6	20		1.10	1.10	1.12	1.14	1.17
CD1D3	10 TO 6	20		1.10	1.11	1.12	1.14	1.17
CD1D4	10 TO 6	20		1.13	1.14	1.16	1.18	1.20
CD2D1	10 TO 6	45		1.12	1.13	1.14	1.16	1.21
CD2D2	10 TO 6	45		1.12	1.12	1.14	1.16	1.18
CD2D3	10 TO 6	45		1.12	1.13	1.14	1.16	1.19
CD2D4	10 TO 6	45		1.14	1.14	1.16	1.17	1.19
CD3D1	10 TO 6	90		1.17	1.16	1.18	1.20	1.21
CD3D2	10 TO 6	90		1.16	1.16	1.17	1.18	1.20
CD3D3	10 TO 6	90		1.17	1.17	1.18	1.20	1.21
CD3D4	10 TO 6	90		1.20	1.20	1.21	1.22	1.23
CD4D1	12 TO 6	20		1.06	1.08	1.08	1.11	1.15
CD4D2	12 TO 6	20		1.07	1.08	1.11	1.13	1.16
CD4D3	12 TO 6	20		1.07	1.08	1.10	1.12	1.14
CD4D4	12 TO 6	20		1.08	1.09	1.11	1.12	1.15
CD5D1	12 TO 6	45		1.11	1.11	1.13	1.15	1.19
CD5D2	12 TO 6	45		1.09	1.10	1.12	1.15	1.17
CD5D3	12 TO 6	45		1.09	1.10	1.12	1.14	1.16
CD5D4	12 TO 6	45		1.10	1.10	1.11	1.13	1.15
CD6D1	12 TO 6	90		1.15	1.15	1.17	1.2	1.2
CD6D2	12 TO 6	90		1.16	1.15	1.17	1.19	1.21
CD6D3	12 TO 6	90		1.16	1.16	1.17	1.19	1.20
CD6D4	12 TO 6	90		1.17	1.16	1.17	1.19	1.19



TABLE 8
Centerline Velocity Data for Round-to-Round Diffusers

Code	Inlet Dia. to Outlet Di Angle (in.) (Deg.)			Velocity Ratio, V_c / V_{avg}				
				1D	2D	4D	6D	10D
DCD1D1	6 TO 10	20		2.27	1.86	1.32	1.19	1.15
DCD1D2	6 TO 10	20		2.26	1.86	1.26	1.13	1.12
DCD1D3	6 TO 10	20		2.36	1.80	1.28	1.14	1.11
DCD1D4	6 TO 10	20		2.40	1.83	1.28	1.17	1.13
DCD2D1	6 TO 10	45		2.59	1.65	1.09	1.05	1.07
DCD2D2	6 TO 10	45		2.59	1.65	1.11	1.08	1.09
DCD2D3	6 TO 10	45		2.55	1.63	1.11	1.08	1.09
DCD2D4	6 TO 10	45		2.81	1.74	1.19	1.11	1.14
DCD3D1	6 TO 10	90		3.46	2.82	1.43	1.13	1.12
DCD3D2	6 TO 10	90		3.42	2.75	1.43	1.13	1.09
DCD3D3	6 TO 10	90		3.35	2.76	1.39	1.11	1.09
DCD3D4	6 TO 10	90		3.46	2.87	1.42	1.15	1.11
DCD4D1	6 TO 12	20		2.79	1.91	1.19	1.08	1.08
DCD4D2	6 TO 12	20		2.86	1.96	1.20	1.07	1.06
DCD4D3	6 TO 12	20		2.81	2.00	1.21	1.08	1.09
DCD4D4	6 TO 12	20		2.83	2.00	1.13	0.96	1.00
DCD5D1	6 TO 12	45		2.36	1.56	1.07	1.09	1.08
DCD5D2	6 TO 12	45		2.25	1.52	1.14	1.09	1.09
DCD5D3	6 TO 12	45		2.41	1.54	1.15	1.11	1.10
DCD5D4	6 TO 12	45		2.53	1.63	1.02	1.02	1.02
DCD6D1	6 TO 12	90		4.87	3.28	1.26	1.02	1.00
DCD6D2	6 TO 12	90		4.81	3.29	1.33	1.10	1.08
DCD6D3	6 TO 12	90		4.05	3.23	1.33	1.09	1.09
DCD6D4	6 TO 12	90		4.93	3.41	1.29	0.97	1.01



TABLE 9
Centerline Velocity Data for Round Diverging Junctions

Code	Dia. of Main Branch (in.)	Dia. of Branch (in.)	Branch Angle (Deg.)	Velocity Ratio, V_c / V_{avg}				
				1D	2D	4D	6D	10D
V2001	10	6	90	0.25	0.66	1.04	1.12	1.12
V2002	10	6	90	0.78	0.78	1.02	1.11	1.12
V2003	10	6	90	0.91	0.85	1.04	1.10	1.12
V2004	10	6	90	0.26	0.54	1.08	1.12	1.08
V2005	10	6	90	0.60	0.67	1.01	1.07	1.06
V2006	10	6	90	0.91	0.78	1.06	1.11	1.09
V2007	10	6	90	0.22	0.55	1.16	1.17	1.08
V2008	10	6	90	0.28	0.66	1.08	1.17	1.15
V2009	10	6	90	0.48	0.70	1.05	1.13	1.12
V2010	10	6	90	0.26	0.58	1.01	1.09	1.08
V2011	12	6	90	0.80	0.74	1.00	1.07	1.09
V2012	12	6	90	1.02	0.82	1.01	1.08	1.11
V2013	12	6	90	0.18	0.35	1.07	1.10	1.07
V2014	12	6	90	0.32	0.61	1.03	1.11	1.10
V2015	12	6	90	0.63	0.69	1.01	1.10	1.11
V2016	12	6	90	0.18	0.32	1.02	1.09	1.02
V2017	12	6	90	0.22	0.64	1.06	1.16	1.14
V2018	12	6	90	0.38	0.65	1.00	1.10	1.10
V3001	16	6	90	0.63	0.62	1.08	1.18	1.18
V3002	16	6	90	1.01	0.73	0.98	1.08	1.10
V3003	16	6	90	1.17	0.74	0.96	1.04	1.08
V3004	16	6	90	0.18	0.47	1.11	1.18	1.18
V3005	16	6	90	0.43	0.59	1.00	1.11	1.09
V3006	16	6	90	1.10	0.65	0.98	1.07	1.08
V3007	16	6	90	0.18	0.32	1.10	1.24	1.14
V3008	16	6	90	0.13	0.52	1.02	1.12	1.08
V3009	16	6	90	0.56	0.63	1.02	1.10	1.07
V4001	10	6	30	1.26	1.23	1.15	1.12	1.10
V4002	10	6	30	1.22	1.11	1.13	1.13	1.12
V4003	10	6	30	1.02	1.04	1.10	1.13	1.12
V4004	10	6	30	1.23	1.22	1.28	1.24	1.13
V4005	10	6	30	1.21	1.18	1.09	1.05	1.05
V4006	10	6	30	1.22	1.15	1.09	1.05	1.05
V4007	10	6	30	1.21	1.39	1.42	1.23	1.08
V4008	10	6	30	1.13	1.13	1.13	1.13	1.15
V4009	10	6	30	1.21	1.18	1.08	1.06	1.04
V5001	12	6	30	1.24	1.19	1.12	1.11	1.12
V5002	12	6	30	1.09	1.02	1.08	1.11	1.10
V5003	12	6	30	0.94	0.98	1.08	1.11	1.11
V5004	12	6	30	1.31	1.29	1.31	1.27	1.13
V5005	12	6	30	1.18	1.14	1.08	1.06	1.07
V5006	12	6	30	1.22	1.13	1.10	1.10	1.11
V5007	12	6	30	1.52	1.52	1.44	1.20	1.08
V5008	12	6	30	1.21	1.23	1.22	1.22	1.17
V5009	12	6	30	1.21	1.18	1.12	1.11	1.11
V6001	16	6	30	1.27	1.22	1.18	1.20	1.20
V6002	16	6	30	0.95	0.99	1.05	1.12	1.13
V6003	16	6	30	0.83	0.90	1.06	1.11	1.12
V6004	16	6	30	1.45	1.41	1.39	1.33	1.23
V6005	16	6	30	1.25	1.20	1.17	1.17	1.14
V6006	16	6	30	1.08	1.02	1.08	1.12	1.13
V6007	16	6	30	1.52	1.61	1.51	1.26	1.15
V6008	16	6	30	1.29	1.27	1.20	1.20	1.18
V6009	16	6	30	1.21	1.18	1.14	1.12	1.10



TABLE 10
Centerline Velocity Data for Round Diverging Wyes Having a 45° Elbow Tap Connection

Code	Dia. of Main Branch (in.)	Dia. of Branch (in.)	Dia. of Inlet Outlet (in.)	Velocity Ratio, V_c / V_{avg}				
				1D	2D	4D	6D	10D
DY1D11	10	6	6	1.12	1.10	1.05	1.04	1.06
DY1D12	10	6	6	1.16	1.13	1.04	1.04	1.08
DY1D13	10	6	6	1.16	1.11	1.04	1.06	1.09
DY1D21	10	6	6	1.22	1.17	1.11	1.17	1.20
DY1D22	10	6	6	1.12	1.09	1.04	1.02	1.05
DY1D23	10	6	6	1.09	1.08	0.99	0.98	1.01
DY1D31	10	6	6	1.14	1.08	1.19	1.29	1.13
DY1D32	10	6	6	1.18	1.14	1.06	1.10	1.15
DY1D33	10	6	6	1.17	1.14	1.10	1.08	1.11
DY2D11	12	6	6	1.17	1.10	1.03	1.00	1.06
DY2D12	12	6	6	1.18	1.15	1.04	1.04	1.07
DY2D13	12	6	6	1.20	1.16	1.04	1.02	1.07
DY2D21	12	6	6	1.16	1.04	1.07	1.24	1.14
DY2D22	12	6	6	1.14	1.08	1.02	1.02	1.07
DY2D23	12	6	6	1.11	1.08	1.01	1.00	1.02
DY2D31	12	6	6	0.81	0.88	1.13	1.19	1.11
DY2D32	12	6	6	1.15	1.14	1.13	1.17	1.14
DY2D33	12	6	6	0.18	1.13	1.06	1.05	1.11
DY3D11	16	6	6	1.19	1.13	1.07	1.05	1.09
DY3D12	16	6	6	1.16	1.11	1.01	1.00	1.03
DY3D13	16	6	6	1.17	1.10	0.98	0.98	1.02
DY3D21	16	6	6	1.20	1.11	1.08	1.20	1.28
DY3D22	16	6	6	1.14	1.10	1.03	1.03	1.09
DY3D23	16	6	6	1.15	1.08	1.00	1.02	1.05
DY3D31	16	6	6	1.19	1.08	1.16	1.25	1.25
DY3D32	16	6	6	1.16	1.09	1.01	1.03	1.10
DY3D33	16	6	6	1.15	1.09	1.02	1.02	1.05



TABLE 11
Centerline Velocity Data for Diverging Junctions with
Rectangular Main and Round Branches

Code	Rect. Main W x H (in.)	Branch Takeoff angle (Deg.)	Tap Conn. Type	Velocity Ratio, V_c / V_{avg}				
				1D	2D	4D	6D	10D
T1D11	8 X 7	30	STR	1.18	1.14	1.01	0.95	0.98
T1D12	8 X 7	30	STR	1.29	1.16	1.09	1.05	1.03
T1D21	8 X 7	30	STR	1.15	1.10	1.16	1.17	1.14
T1D22	8 X 7	30	STR	1.21	1.15	1.03	0.96	0.99
T1D23	8 X 7	30	STR	1.26	1.17	1.10	1.05	1.03
T1D31	8 X 7	30	STR	0.96	1.05	1.31	1.32	1.10
T1D32	8 X 7	30	STR	1.10	1.07	1.00	1.02	1.06
T1D33	8 X 7	30	STR	1.21	1.16	1.03	0.98	0.98
T2D11	12 X 10	30	STR	1.22	1.21	1.17	1.15	1.15
T2D12	12 X 10	30	STR	1.31	1.12	1.11	1.14	1.12
T2D13	12 X 10	30	STR	1.28	1.07	1.09	1.14	1.12
T2D21	12 X 10	30	STR	1.51	1.41	1.31	1.21	1.09
T2D22	12 X 10	30	STR	1.21	1.21	1.16	1.15	1.13
T2D23	12 X 10	30	STR	1.28	1.17	1.11	1.13	1.15
T2D31	12 X 10	30	STR	1.69	1.75	1.38	1.14	1.08
T2D32	12 X 10	30	STR	1.34	1.31	1.26	1.19	1.13
T2D33	12 X 10	30	STR	1.21	1.20	1.17	1.14	1.12
T3D11	18 X 10	30	STR	1.17	1.17	1.14	1.14	1.11
T3D12	18 X 10	30	STR	1.26	1.08	1.07	1.11	1.12
T3D13	18 X 10	30	STR	1.26	1.04	1.08	1.12	1.10
T3D21	18 X 10	30	STR	1.40	1.36	1.31	1.23	1.11
T3D22	18 X 10	30	STR	1.17	1.17	1.17	1.15	1.13
T3D23	18 X 10	30	STR	1.21	1.14	1.09	1.11	1.12
T3D31	18 X 10	30	STR	1.48	1.53	1.32	1.15	1.05
T3D32	18 X 10	30	STR	1.30	1.28	1.24	1.22	1.13
T3D33	18 X 10	30	STR	1.16	1.16	1.16	1.15	1.12

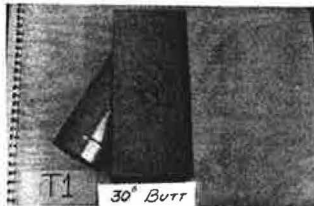


TABLE 11
Centerline Velocity Data for Diverging Junctions with
Rectangular Main and Round Branches (Continued)

Code	Rect. Main W x H (in.)	Branch Takeoff angle (Deg.)	Tap Conn. Type	Velocity Ratio, V_c / V_{avg}				
				1D	2D	4D	6D	10D
T7D11	8 X 7	30	CON	1.00	0.95	0.92	0.95	1.02
T7D12	8 X 7	30	CON	1.11	1.06	0.96	1.01	1.06
T7D21	8 X 7	30	CON	0.88	0.91	1.01	1.11	1.10
T7D22	8 X 7	30	CON	1.01	0.95	0.93	0.98	1.03
T7D23	8 X 7	30	CON	1.09	1.01	0.95	0.99	1.05
T7D31	8 X 7	30	CON	0.94	0.97	1.21	1.20	1.09
T7D32	8 X 7	30	CON	0.95	0.92	0.98	1.04	1.09
T7D33	8 X 7	30	CON	1.02	0.96	0.94	0.99	1.04
T8D11	12 X 10	30	CON	1.11	1.09	1.07	1.10	1.11
T8D12	12 X 10	30	CON	1.10	1.10	1.09	1.08	1.05
T8D13	12 X 10	30	CON	1.12	1.09	1.09	1.10	1.04
T8D21	12 X 10	30	CON	1.25	1.24	1.26	1.23	1.13
T8D22	12 X 10	30	CON	1.12	1.10	1.07	1.08	1.09
T8D23	12 X 10	30	CON	1.09	1.09	1.08	1.08	1.04
T8D31	12 X 10	30	CON	1.40	1.44	1.31	1.16	1.06
T8D32	12 X 10	30	CON	1.15	1.13	1.14	1.17	1.15
T8D33	12 X 10	30	CON	1.11	1.08	1.07	1.07	1.08
T9D11	18 X 10	30	CON	1.08	1.05	1.03	1.03	1.07
T9D12	18 X 10	30	CON	1.09	1.09	1.09	1.09	1.05
T9D13	18 X 10	30	CON	1.11	1.11	1.11	1.11	1.07
T9D21	18 X 10	30	CON	1.15	1.11	1.15	1.18	1.13
T9D22	18 X 10	30	CON	1.09	1.05	1.04	1.05	1.08
T9D23	18 X 10	30	CON	1.09	1.09	1.08	1.07	1.05
T9D31	18 X 10	30	CON	1.32	1.35	1.31	1.15	1.05
T9D32	18 X 10	30	CON	1.08	1.07	1.09	1.12	1.12
T9D33	18 X 10	30	CON	1.07	1.02	1.02	1.03	1.06



TABLE 11
Centerline Velocity Data for Diverging Junctions with
Rectangular Main and Round Branches (Continued)

Code	Rect. Main W x H (in.)	Branch Takeoff angle (Deg.)	Tap Conn. Type	Velocity Ratio, V_c / V_{avg}				
				1D	2D	4D	6D	10D
T10D11	8 X 7	90	CON	0.57	0.70	0.96	1.03	1.07
T10D12	8 X 7	90	CON	0.75	0.84	0.97	1.04	1.04
T10D21	8 X 7	90	CON	0.26	0.54	0.99	1.09	1.08
T10D22	8 X 7	90	CON	0.58	0.72	0.96	1.05	1.08
T10D23	8 X 7	90	CON	0.70	0.77	0.96	1.03	1.03
T10D31	8 X 7	90	CON	0.19	0.39	0.97	1.11	1.08
T10D32	8 X 7	90	CON	0.39	0.63	0.97	1.07	1.08
T10D33	8 X 7	90	CON	0.58	0.74	0.98	1.06	1.08
T11D11	12 X 10	90	CON	0.69	0.73	0.93	1.00	1.04
T11D12	12 X 10	90	CON	0.83	0.80	0.92	0.99	1.03
T11D13	12 X 10	90	CON	0.95	0.85	0.96	1.01	1.05
T11D21	12 X 10	90	CON	0.48	0.70	0.98	1.09	1.08
T11D22	12 X 10	90	CON	0.74	0.76	0.93	1.01	1.04
T11D23	12 X 10	90	CON	0.81	0.77	0.91	0.98	1.04
T11D31	12 X 10	90	CON	0.22	0.67	1.06	1.12	1.07
T11D32	12 X 10	90	CON	0.61	0.72	0.97	1.07	1.08
T11D33	12 X 10	90	CON	0.74	0.75	0.93	1.02	1.07
T12D11	18 X 10	90	CON	0.94	0.86	0.93	1.02	1.03
T12D12	18 X 10	90	CON	1.13	0.87	0.91	0.98	1.01
T12D13	18 X 10	90	CON	1.05	0.89	0.93	1.00	1.03
T12D21	18 X 10	90	CON	1.13	1.12	1.10	1.16	1.10
T12D22	18 X 10	90	CON	0.94	0.85	0.91	1.01	1.04
T12D23	18 X 10	90	CON	0.96	0.86	0.92	0.98	1.04
T12D31	18 X 10	90	CON	1.56	1.38	1.35	1.31	1.07
T12D32	18 X 10	90	CON	1.07	1.00	1.04	1.09	1.09
T12D33	18 X 10	90	CON	0.96	0.90	0.95	1.04	1.04



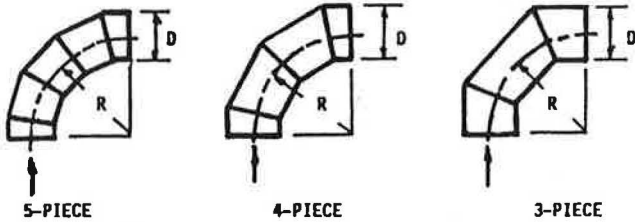
TABLE 11
Centerline Velocity Data for Diverging Junctions with
Rectangular Main and Round Branches (Continued)

Code	Rect. Main W x H (in.)	Branch Takeoff angle (Deg.)	Tap Conn. Type	Velocity Ratio, V_c / V_{avg}				
				1D	2D	4D	6D	10D
T4D11	8 X 7	90	STR	0.45	0.47	0.94	1.06	1.04
T4D12	8 X 7	90	STR	1.09	0.63	0.94	1.05	1.08
T4D21	8 X 7	90	STR	0.18	0.23	0.88	1.07	1.08
T4D22	8 X 7	90	STR	0.19	0.35	0.91	1.02	1.04
T4D23	8 X 7	90	STR	0.81	0.57	0.97	1.08	1.09
T4D31	8 X 7	90	STR	0.18	0.26	0.83	1.05	1.07
T4D32	8 X 7	90	STR	0.11	0.29	0.93	1.05	1.07
T4D33	8 X 7	90	STR	0.34	0.36	0.94	1.05	1.04
T5D11	12 X 10	90	STR	0.43	0.32	0.90	1.05	1.04
T5D12	12 X 10	90	STR	1.02	0.56	0.90	1.02	1.07
T5D13	12 X 10	90	STR	1.13	0.71	0.89	1.02	1.07
T5D21	12 X 10	90	STR	0.18	0.24	0.98	1.09	1.03
T5D22	12 X 10	90	STR	0.59	0.44	0.91	1.07	1.07
T5D23	12 X 10	90	STR	0.96	0.61	0.92	1.06	1.06
T5D31	12 X 10	90	STR	0.18	0.18	0.94	1.11	1.03
T5D32	12 X 10	90	STR	0.25	0.27	0.91	1.10	1.04
T5D33	12 X 10	90	STR	0.60	0.45	0.93	1.06	1.06
T6D11	18 X 10	90	STR	0.71	0.43	0.97	1.12	1.10
T6D12	18 X 10	90	STR	1.19	0.64	0.94	1.08	1.08
T6D13	18 X 10	90	STR	1.31	0.73	0.89	1.02	1.08
T6D21	18 X 10	90	STR	0.18	0.26	1.06	1.13	1.07
T6D22	18 X 10	90	STR	0.61	0.38	0.97	1.07	1.04
T6D23	18 X 10	90	STR	1.18	0.66	0.99	1.11	1.11
T6D31	18 X 10	90	STR	0.18	0.23	1.04	1.12	1.08
T6D32	18 X 10	90	STR	0.17	0.33	1.04	1.11	1.08
T6D33	18 X 10	90	STR	0.75	0.43	0.98	1.09	1.06



TABLE 12
Ratio of Average Velocity from Pitot Traverse to Average Velocity from Independently Measured Flow Rate
(Selected Elbow Cases)

Traverse Position	Traverse Plane	Fitting Test Code Number			
		E1D2	E13D2	E19D2	E31D2
1D	V	1.118	1.158	1.164	1.102
	H	0.964	0.929	0.845	0.849
2D	V	1.082	1.086	1.100	1.085
	H	1.017	1.006	0.970	0.944
4D	V	1.065	1.063	1.068	1.045
	H	1.043	1.021	1.013	0.988
6D	V	1.057	1.062	1.061	1.040
	H	1.043	1.009	1.026	0.974
10D	V	1.048	0.971	1.049	1.015
	H	1.033	1.026	1.021	1.001

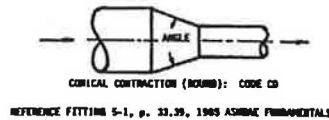


ELBOWS: CODE E

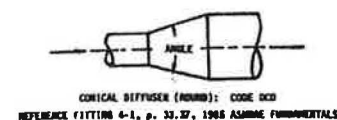
REFERENCE FITTING 3-2, p. 33.33, 1985 ASHRAE FUNDAMENTALS

TABLE 13
Ratio of Average Velocity from Pitot Traverse to Average Velocity from Independently Measured Flow Rate
(Selected Contraction and Diffuser Cases)

Traverse Position	Traverse Plane	Fitting Test Code Number			
		Diffusers		Contractions	
		DCD4D2	DCD6D2	CD4D2	CD6D2
1D	V	1.232	1.300	1.029	1.011
	H	1.158	1.406	1.013	1.021
2D	V	1.184	1.217	1.029	1.022
	H	1.146	1.277	1.015	1.018
4D	V	1.052	1.102	1.033	1.036
	H	1.079	1.115	1.021	1.024
6D	V	1.021	1.043	1.038	1.046
	H	1.029	1.053	1.020	1.029
10D	V	1.003	1.012	1.034	1.042
	H	1.005	1.009	1.009	1.019



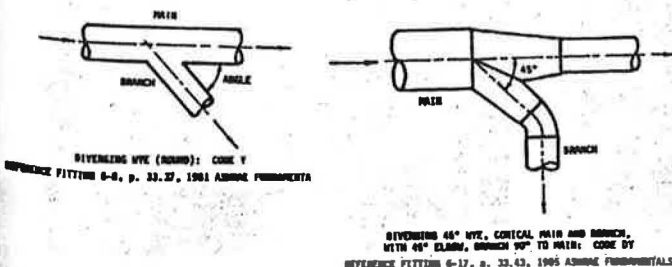
REFERENCE FITTING 5-1, p. 33.39, 1985 ASHRAE FUNDAMENTALS



REFERENCE FITTING 4-1, p. 33.37, 1985 ASHRAE FUNDAMENTALS

TABLE 14
Ratio of Average Velocity from Pitot Traverse to Average Velocity from Independently Measured Flow Rate
(Selected Y and DY Cases)

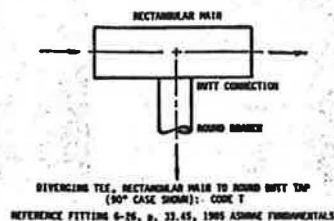
Traverse Position	Traverse Plane	Fitting Test Code Number			
		Y's		DY's	
		Y1D22 (90 Deg.)	Y4D22 (30 Deg.)	DY1D22	DY3D22
1D	V	1.447	1.137	1.126	1.187
	H	0.888	0.929	0.946	0.980
2D	V	1.226	1.130	1.075	1.154
	H	0.890	0.970	0.937	1.028
4D	V	1.075	1.120	1.043	1.117
	H	1.003	0.997	0.989	1.048
6D	V	1.023	1.105	1.036	1.104
	H	1.002	1.018	1.003	1.058
10D	V	0.979	1.071	1.029	1.081
	H	0.979	1.036	0.998	1.049



REFERENCE FITTING 6-17, p. 33.43, 1985 ASHRAE FUNDAMENTALS

TABLE 15
Average Velocity Ratios on the Basis of Equal Area
(Selected Tee Cases)

Traverse Position	Traverse Plane	Fitting Test Code Number			
		Straight Tap			
		T1D22	T3D22	T4D22	T6D22
1D	V	1.088	1.062	1.149	1.258
	H	0.902	0.928	0.877	0.951
2D	V	1.077	1.068	1.126	1.204
	H	0.921	0.934	0.853	0.847
4D	V	1.056	1.064	1.045	1.025
	H	0.939	0.978	0.993	1.055
6D	V	1.037	1.051	1.003	0.986
	H	0.953	1.002	0.990	1.039
10D	V	1.015	1.004	0.972	0.971
	H	0.971	1.015	0.976	0.982



REFERENCE FITTING 6-26, p. 33.45, 1985 ASHRAE FUNDAMENTALS

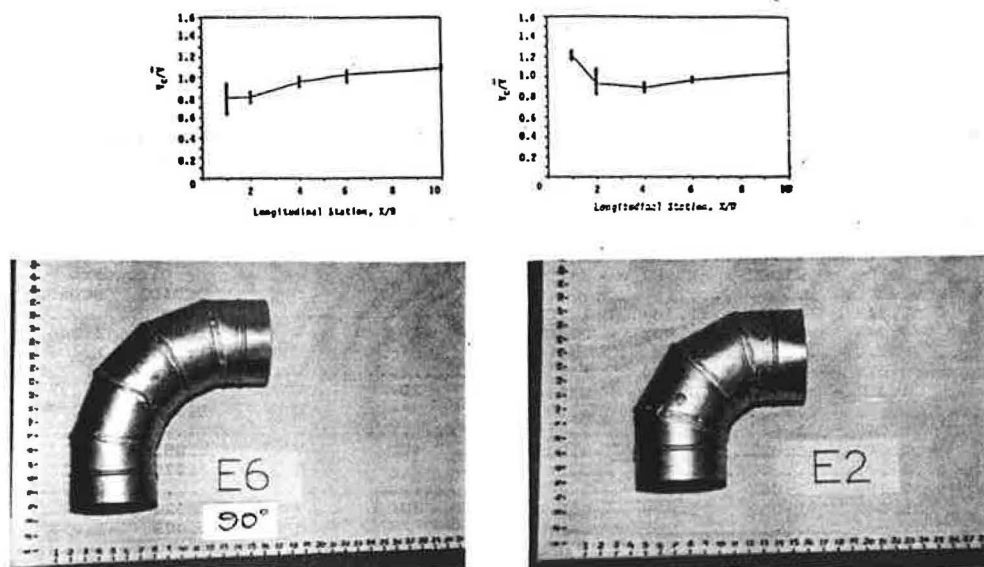


Figure 2 Centerline velocity data for elbows (a) 90°; (b) 45°

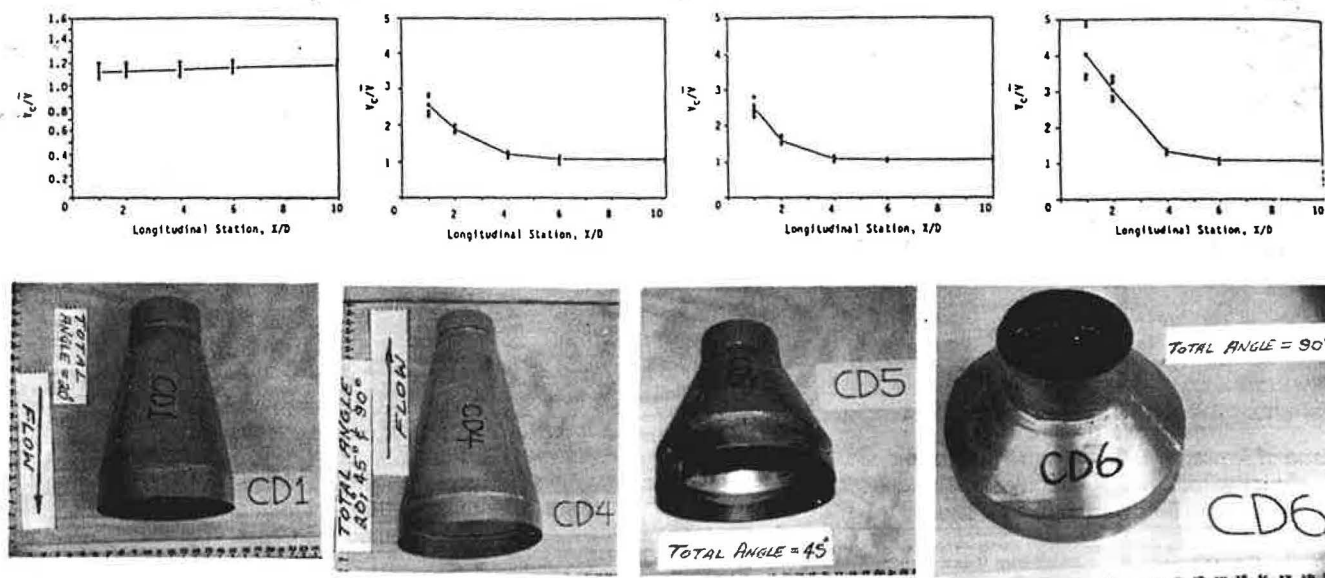


Figure 3 Centerline velocity data for contractions and diffusers
(a) all contractions (CDs); (b) 20° diffuser (DCD1 and DCD4);
(c) 45° diffuser (DCD2 and DCD5); (d) 90° diffuser (DCD3 and DCD6)

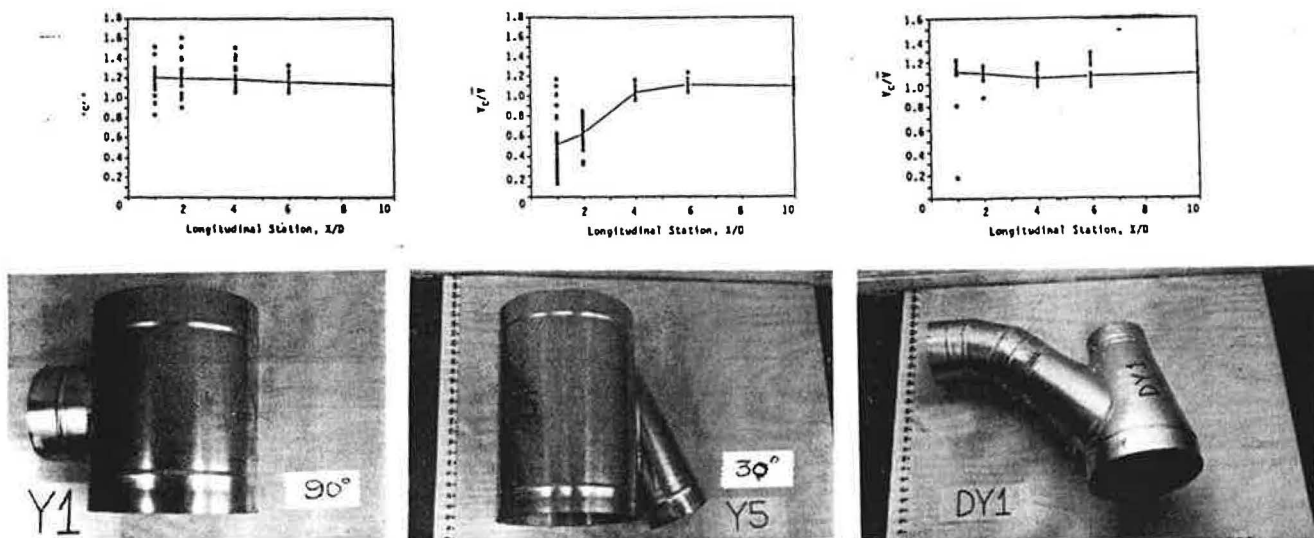


Figure 4 Centerline velocity data for round-to-round junctions (a) 90°; (b) 30°; (c) all DY's

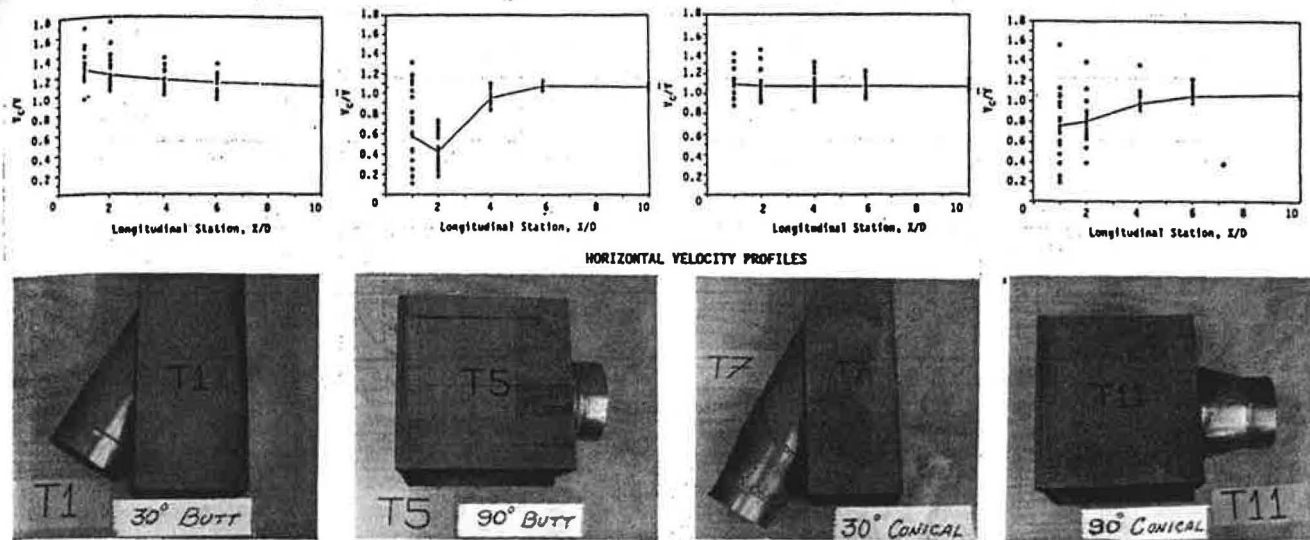


Figure 5 Centerline velocity data for rectangular-to-round junctions
(a) 30° butt tap; (b) 90° butt tap; (c) 30° conical tap; (d) 90° conical tap

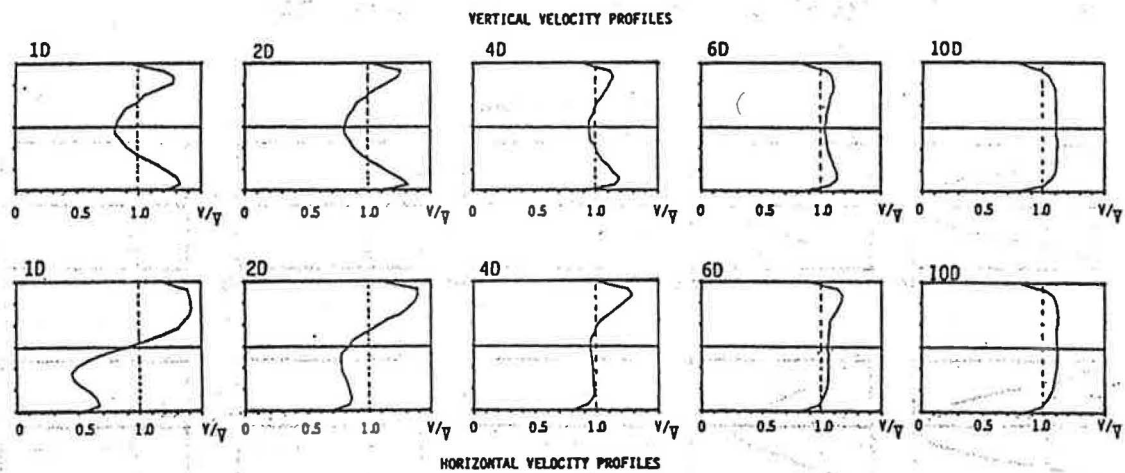


Figure 6 Depiction of profile evolution for test case E2D2

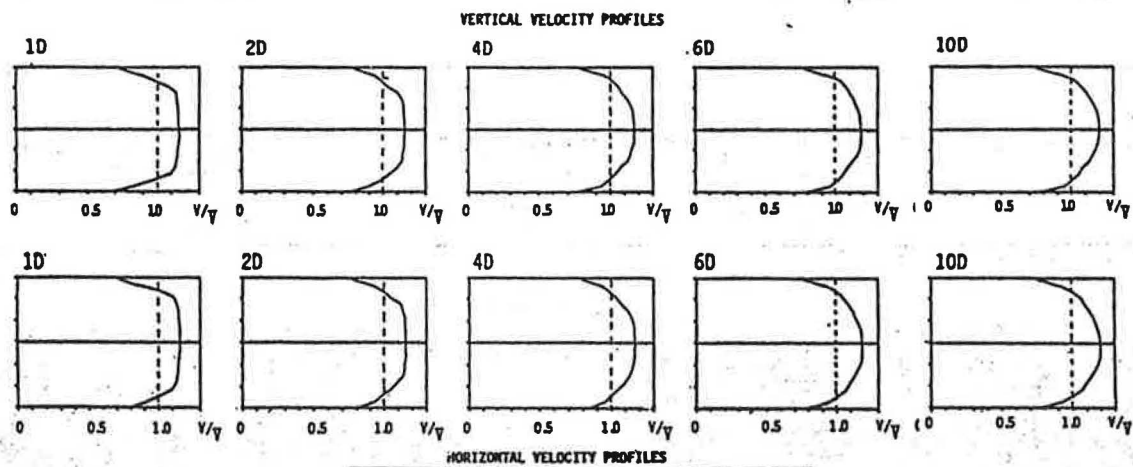


Figure 7 Depiction of profile evolution for test case CD3D2

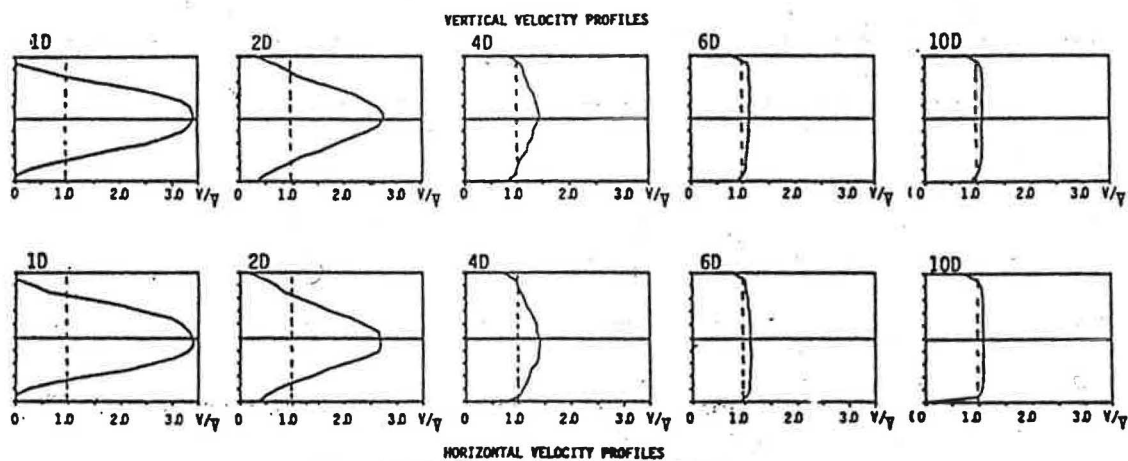


Figure 8 Depiction of profile evolution for test case DCD3D2

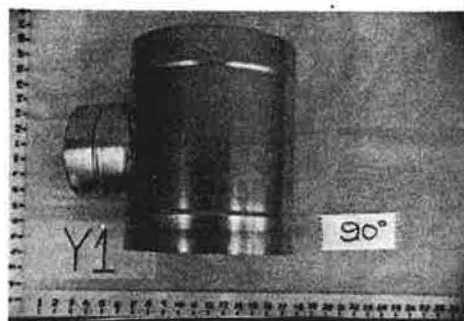
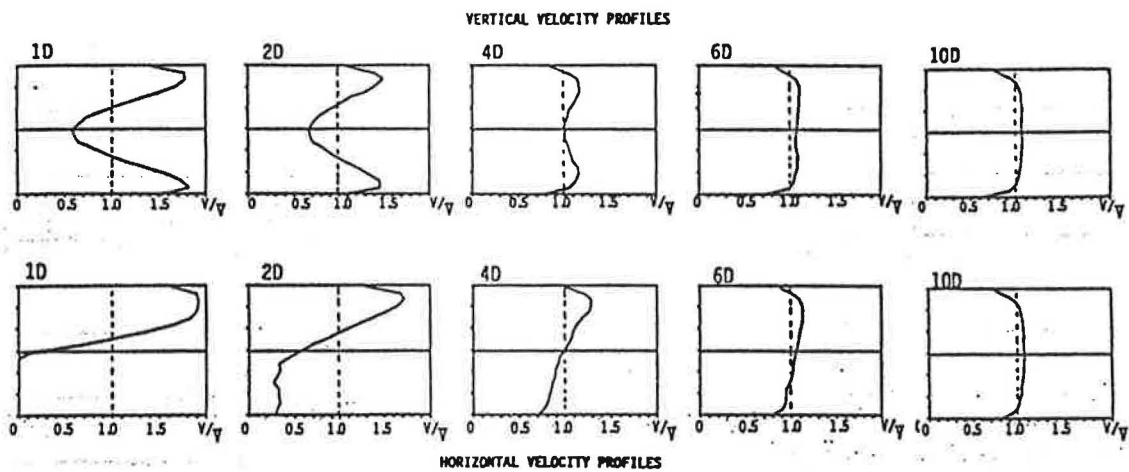


Figure 9 Depiction of profile evolution for test case Y1D22

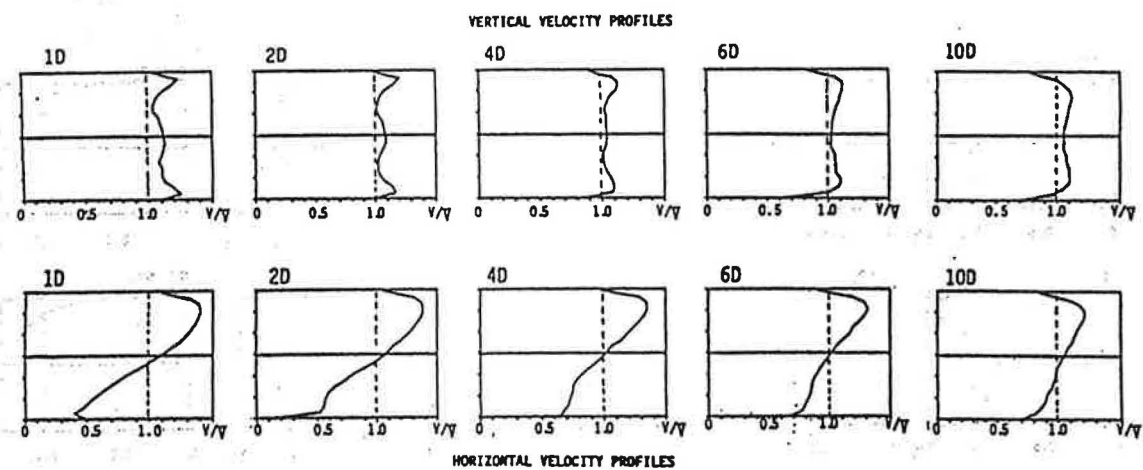


Figure 10 Depiction of profile evolution for test case DY1D22

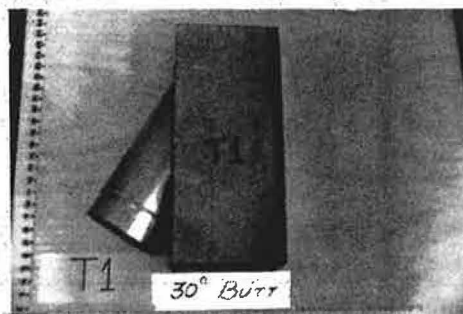
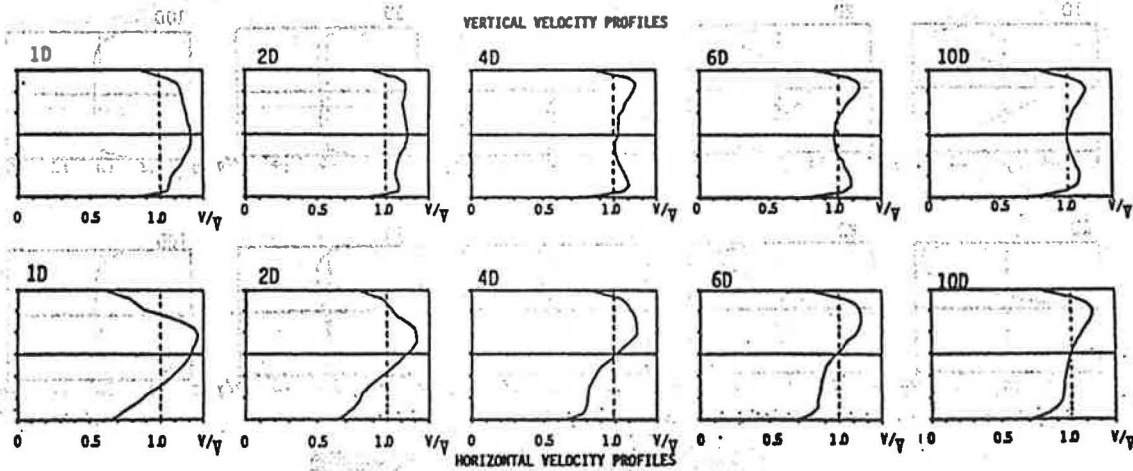


Figure 11 Depiction of profile evolution for test case T1D22

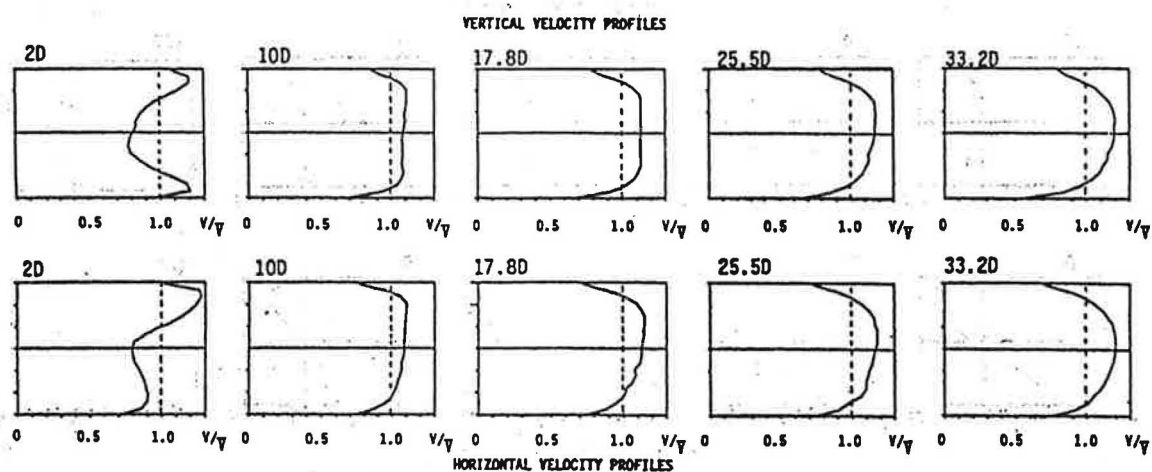


Figure 12 Depiction of profile evolution for test case E6D22 with extended downstream measuring stations

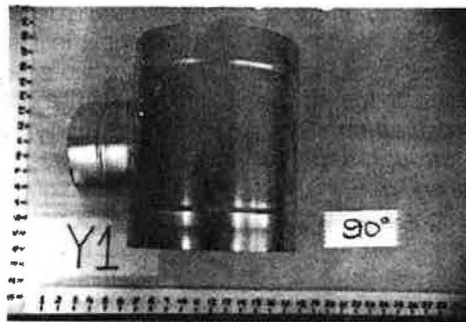
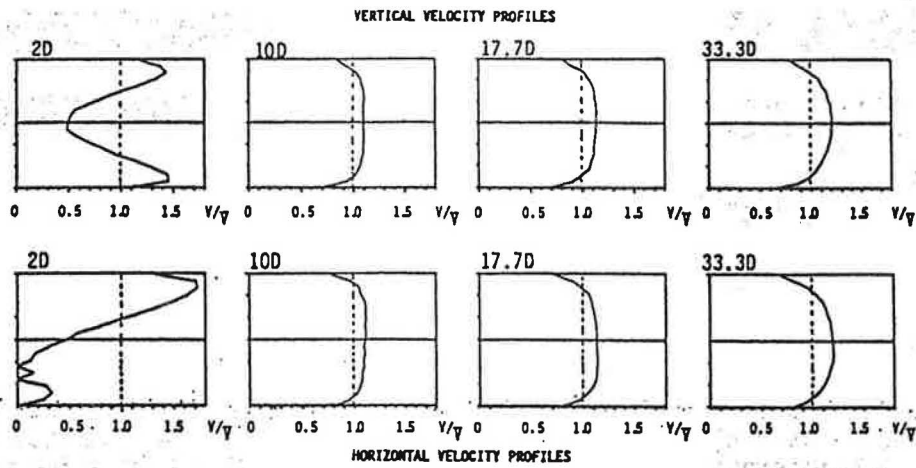


Figure 13 Depiction of profile evolution for test case Y1D22 with extended downstream measuring stations